Deterministic constrained synthesis technique for conformal aperiodic linear antenna arrays - Part II

Deterministic Constrained Synthesis Technique for Conformal Aperiodic Linear Antenna Arrays—Part II: Applications

Diego Caratelli, *Senior Member, IEEE*, Giovanni Toso, *Senior Member, IEEE*, Oleg V. Stukach, *Senior Member, IEEE*, and Nikolay V. Panokin

***Abstract*— The aim of this paper is to illustrate the application of the antenna placement methodology introduced in Part I for the deterministic synthesis of general conformal aperiodic arrays subject to multiple concurrent design constraints on the relevant layout and excitation tapering, as it is typically the case in satellite communications and radar applications. Antenna mutual coupling is not considered in the developed methodology; hence, to assess the sensitivity of the design procedure to such nonideality, a dedicated investigation has been conducted using rigorous full-wave electromagnetic modeling and experimental measurements collected on physical prototypes. The obtained results demonstrate the effectiveness and versatility of the proposed array synthesis approach, even in operative scenarios in which a significant deviation from the desired antenna operation is observed.**

***Index Terms*— Antenna arrays, antenna radiation patterns, antenna theory, antennas, electromagnetic measurements, electromagnetic modeling, evolutionary computation, mutual coupling, satellite antennas, synthetic aperture radar (SAR).**

I. Introduction

CONFORMAL antenna array synthesis and analysis are of paramount importance for designing modern radar and satellite communication systems [1]–[3]. Particularly attractive in this regard is the use of sparse array topologies, by means of which it is possible to reduce the overall number of embedded radiating elements without a significant degradation of the radiation pattern characteristics compared to conventional uniformly spaced array architectures while achieving, on the other hand, substantial benefits in terms of system complexity and manufacturing costs [4]–[12].

The analysis of conformal antenna arrays can be undertaken using a variety of approaches depending on whether the array dimensions are small with respect to the curvature radius of the antenna platform or the platform itself is large or small with respect to the operating wavelength [13], [14]. Full-wave numerical modeling based on the method of moments (MoM), finite-element method (FEM), or finite-difference time-domain (FDTD) techniques [15], [16] is not practically applied for electrically large host bodies, and to date, hybrid approaches relying on asymptotic techniques, such as physical optics (PO) [17] and uniform theory of diffraction (UTD) [18], have proved to be more effective for bulkier structures. Nevertheless, the nonnegligible computational burden of the aforementioned electromagnetic modeling schemes makes them unsuitable for directly addressing complex radiation pattern synthesis problems.

The synthesis of general sparse conformal antenna arrays is a challenging problem because of its nonconvexity and the strong nonlinearity between the electromagnetic field distribution in Fraunhofer region and the unknowns, primarily, the number of positions of the array elements. Therefore, where local optimization algorithms [19] are adopted in the design procedure, these are likely to be trapped into local minima. The use of global minimization techniques, such as stochastic evolutionary algorithms [20]–[25], allows asymptotically obtaining the optimal solution of the problem but at the expense of a significant synthesis time that increases exponentially as the number of unknowns becomes large [26], [27]. In order to overcome the aforementioned drawbacks, the deterministic synthesis methodology presented in Part I of this paper [28] can be used. In this way, by making judicious use of the auxiliary array pattern (AAP) theory [29]–[31], the design problem can be reduced to a convex routine, with the inherent advantages in terms of computational time and solution optimality. By applying the developed procedure, one can readily determine the optimal aperiodic array architecture featuring a radiation pattern consistent with an arbitrary assigned mask. An extensive numerical study will prove the effectiveness of the proposed approach.

Array analysis and synthesis involve an additional complication in which the parasitic electromagnetic interaction

Manuscript received December 8, 2017; revised March 5, 2019; accepted April 27, 2019. Date of publication May 20, 2019; date of current version September 4, 2019. This work was in part funded by The Antenna Company through the European Space Agency under Contract 4000115462/15/NL/AF and in part supported by the National University of Science and Technology MISiS and Tomsk Polytechnic University through the Competitiveness Enhancement Program. *(Corresponding author: Diego Caratelli.)*

D. Caratelli is with the Department of Research and Development, The Antenna Company, 5656 AE Eindhoven, The Netherlands, also with the Institute of Cybernetics, Tomsk Polytechnic University, 634050 Tomsk, Russia, and also with the Electromagnetics Group, Department of Electrical Engineering, Eindhoven University of Technology, 5600 MB Eindhoven, The Netherlands (e-mail: diego.caratelli@antennacompany.com).

G. Toso is with the Antenna and Sub-Millimeter Wave Section, Electromagnetics Division, European Space Agency, 2200 AG Noordwijk, The Netherlands (e-mail: giovanni.toso@esa.int).

O. V. Stukach is with the School of Electronic Engineering, Tikhonov Institute of Electronics and Mathematics, National Research University Higher School of Economics, 101000 Moscow, Russia (e-mail: ostukach@hse.ru).

N. V. Panokin is with the Center of Intelligent Autonomous Systems, National University of Science and Technology MISiS, 119049 Moscow, Russia (e-mail: n.panokin@misis.ru).

Color versions of one or more of the figures in this article are available online at http://ieeexplore.ieee.org.

Digital Object Identifier 10.1109/TAP.2019.2916675

between radiating elements must be considered [32]–[35]. Depending on the specific application, antenna mutual coupling can affect the array performance in terms of radiation properties, signal-to-interference-and-noise ratio (SINR), radar cross section (RCS) resolution, and direction-of-arrival (DOA) estimation accuracy. This problem also depends on the host body dimensions and relative curvature [36], [37]. In the presented formulation, the effect of mutual coupling between the antennas is not directly embedded, although this point can be properly handled in combination with the theory of active element pattern (AEP), as presented in [38] and [39]. To assess the sensitivity of the proposed synthesis tool to the aforementioned antenna nonideality, a dedicated numerical investigation is conducted using a full-wave electromagnetic solving technique. Additionally, an experimental validation is performed using measurements collected on physical prototypes.

This paper is organized as follows. Section II validates the developed antenna placement technique via its application to the synthesis of conformal aperiodic arrays featuring complex radiation pattern masks for satellite communications and radar applications. Section III summarizes the conclusions.

II. Application of the Array Synthesis Procedure

In this section, the proposed antenna placement technique is validated by applying it to the synthesis of complex conformal aperiodic arrays integrated on circular platforms, subject to design constraints that are often encountered in radar and space applications.

A. Synthesis of a Pencil-Beam Arc Antenna Array

1) Design Problem: We first consider the problem of synthesizing a linear aperiodic circular arc array with a pencil-beam radiation pattern [40] characterized by half-power beamwidth (HPBW) $\Theta_0 = 6^\circ$ and peak sidelobe level (PSL) $\varsigma_p = -20$ dB under the constraint of maximal aperture $L_a = 24\,\lambda_0$ and minimum interelement spacing $d_{\min} = 2\,\lambda_0/3$, with λ_0 the free-space wavelength. In addition, the targeted radiated field mask $F_O(\varphi)$ is prescribed to feature the following phase distribution in the main lobe region:

$$\arg\{F_O(\varphi)\} = \pi \mid \varphi/\Theta_0|^3. \tag{1}$$

2) Synthesis Neglecting Antenna Coupling: Under the assumption that the array elements display, along the azimuthal observation plane $\vartheta = \theta_0 = \pi/2$, uniform radiation pattern characteristics with $f(\psi_a, \theta_0, \varphi) \backsimeq 1$, the synthesis procedure detailed in [28, Sec. II-B] is applied to evaluate the array taper function (ATF) $\gamma(\upsilon)$ for different normalized curvature radii R_a/λ_0 of the radiating structure (see Fig. 1). As R_a increases (and the antenna platform tends to collapse on a plane), the amplitude taper, which is directly related to $|\gamma(\upsilon)|$, shows a progressively larger correlation degree with the excitation profile of a Dolph–Chebyshev array [41] with the same HPBW and PSL, as it is shown in Fig. 2.

In the following, attention is focused on the architecture with radius $R_a = 30\,\lambda_0$. In this case, by enforcing the aforementioned design constraint on the minimum antenna separation, the angular element density $\Phi(q)$ (see Fig. 3) can be determined along with the array amplitude and phase excitation functions $A(q)$ and $\alpha(q)$ from [28, eq. (24)] and [28, eq. (25)], respectively. This observation, in turn, directly translates into the ability to evaluate the relevant AAP in

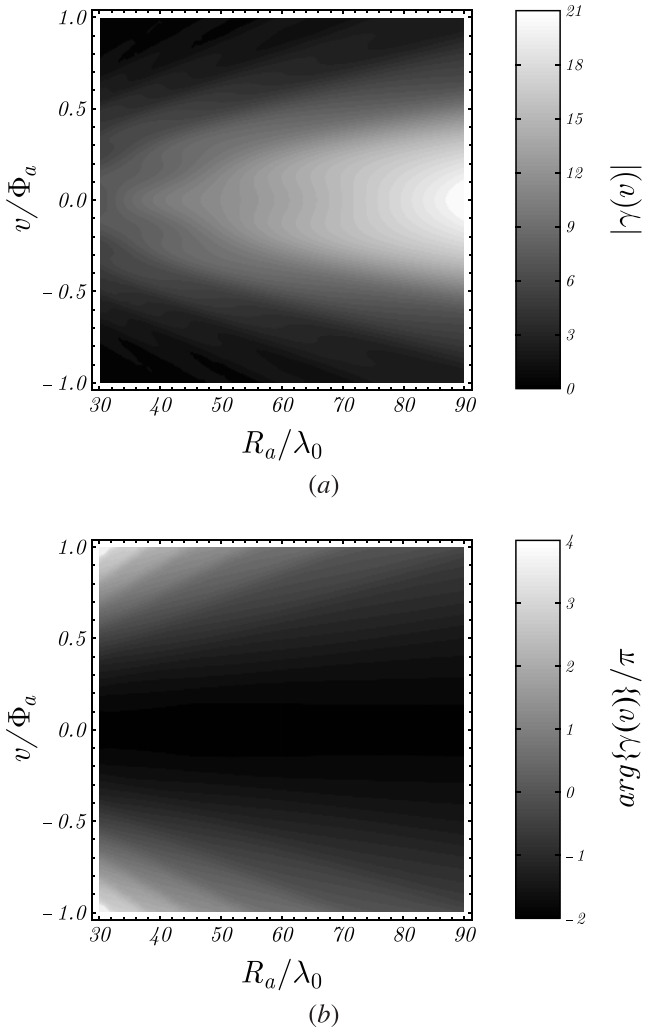

Fig. 1. (a) Magnitude and (b) phase of the taper distribution $\gamma(\upsilon)$ relevant to a pencil-beam arc array of aperture $L_a = 24\,\lambda_0$ as a function of the normalized radius R_a/λ_0 of the circular platform on which the radiating structure is integrated.

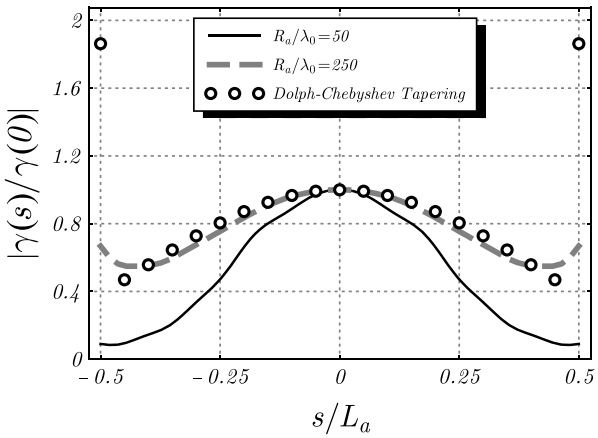

Fig. 2. Normalized amplitude tapering of a pencil-beam arc array of aperture $L_a = 24\,\lambda_0$ as a function of the curvilinear abscissa $s = R_a\upsilon$, with $\upsilon \in [-\Phi_a, \Phi_a]$, for different curvature radii R_a of the host platform.

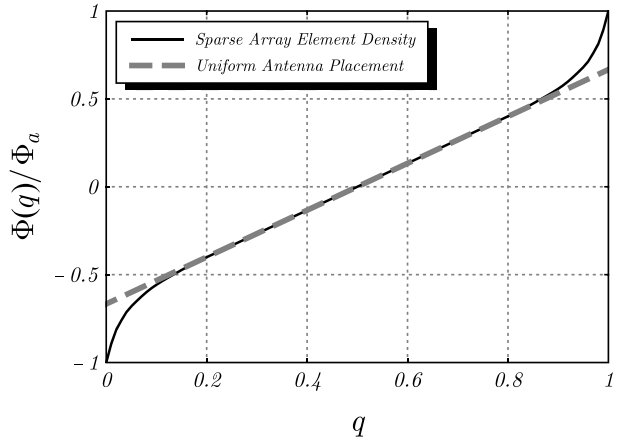

Fig. 3. Angular element density of a pencil-beam arc array of aperture $L_a = 24\,\lambda_0$ and curvature radius $R_a = 30\,\lambda_0$ subject to the design constraint on minimum antenna separation $d_{\min} = 2\,\lambda_0/3$.

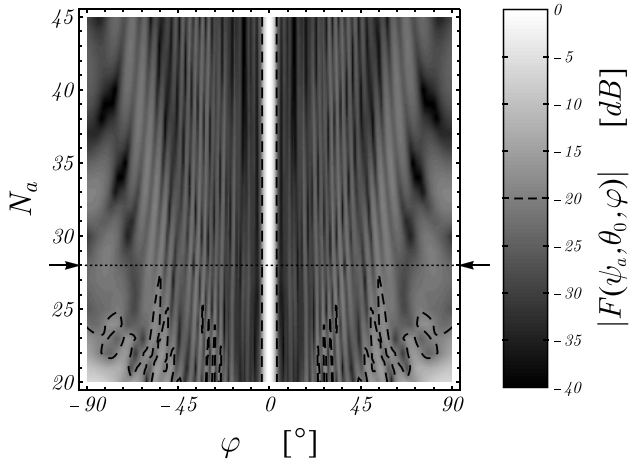

Fig. 4. Magnitude of the radiated electric field of a pencil-beam arc array of aperture $L_a = 24\,\lambda_0$ and curvature radius $R_a = 30\,\lambda_0$ as a function of the azimuthal observation angle φ and number N_a of antenna elements.

[28, eq. (3)]. As shown in Fig. 4, the minimal number of antennas that are required to meet the assigned specification in terms of PSL for the considered design problem is $N_a = 28$. The resulting array characteristics, which are obtained by indicial sampling of the continuous illumination functions, are shown in Fig. 5, whereas the optimal antenna placement is shown in Fig. 6(a). In this manner, we determine that the achieved minimum interelement spacing is $\Delta s_{\min} = 0.67\,\lambda_0$, with the average antenna separation being about $0.86\,\lambda_0$. Finally, a visual inspection of Fig. 7 shows that both the magnitude and the phase of the synthesized array pattern accurately follow the prescribed radiation mask.

3) Synthesis Considering Antenna Coupling: The detrimental effect of spurious mutual antenna coupling has been neglected so far in the considered test case. Therefore, to assess the sensitivity of the proposed design methodology to the aforementioned nonideality, a dedicated numerical investigation was performed. To this end, the radiation properties of the synthesized linear sparse array consisting of N_a identical perfectly conducting cylindrical dipoles [see Fig. 6(b)] were rigorously analyzed using the locally conformal FDTD scheme presented in [42] and [43]. This procedure allows for the modeling of complex shaped electromagnetic structures while avoiding the staircase approximation of the relevant geometry, thereby providing an advantage in terms of accuracy over the use of the conventional Yee algorithm as well as unstructured or stretched space lattices that potentially suffer from numerical dispersion and instability [44].

TABLE I

COMPUTATIONAL BURDEN OF ALTERNATIVE DESIGN METHODOLOGIES FOR SYNTHESIZING A LINEAR APERIODIC CIRCULAR ARC ARRAY

Array Synthesis Methodology	Computational Time (s)	Memory Usage (MB)
Evolutionary PSO-based Algorithm [47]	9567.765	99.917
Proposed Deterministic Technique	27.994	12.727

The length, radius, and feeding delta gap of the individual dipole were selected as $l_d = 0.425\,\lambda_0$, $r_d = 0.0125\,\lambda_0$, and $\delta_d = 0.005\,\lambda_0$, respectively, to achieve good performance in terms of return loss (with respect to the reference impedance $Z_0 = 50\ \Omega$) in the array configuration, namely, $|S_{ii}| \lesssim -13.7$ dB ($i = 1, 2, \ldots, N_a$) at the central working frequency $f_0 = c_0/\lambda_0$, where c_0 denotes the speed of light in free space [see Fig. 8(a)]. Under such assumptions, the maximum spurious coupling level between the radiating elements was found to be $\max_{i \neq j} |S_{ij}(f_0)| \simeq -15.3$ dB [see Fig. 8(b)], whereas the average AEP

$$f_e(\psi_a, \vartheta, \varphi) = \frac{1}{N_a} \sum_{n=1}^{N_a} f_n(\psi_a, \vartheta, \varphi + \bar{\Phi}_n) \tag{2}$$

features the angular behavior shown in Fig. 9 along the azimuthal observation plane $\vartheta = \theta_0 = \pi/2$. It was determined that $|f_e(\psi_a, \theta_0, \varphi)| \simeq 1 + 3\,(\cos\varphi)^8/4$, which results in a nonmarginal deviation from the ideal operation. As a matter of fact, the electromagnetic scattering processes occurring among the elements of the array unavoidably affect the behavior of the antenna in its array environment compared to that of the radiator taken in isolation. In the specific test case, the impact can be measured in a shift up to about 1.95% in the fundamental resonant frequency f_0 of the individual dipole due to the loading effect of adjacent radiating elements. Obviously, the severity of the problem becomes larger in dense regular arrays, where interelement spacing is kept smaller than half wavelength to avoid grating lobes while scanning. The adoption of irregular array architectures, on the other hand, may mitigate this issue because of the additional control that is introduced, at design stage, on the antenna separation and, therefore, tolerable parasitic coupling level.

Despite the aforementioned nonidealities, the angular behavior of the synthesized array pattern is not severely impacted by parasitic processes as shown in Fig. 7, with the level of the first sidelobes slightly increasing but remaining well below the assigned amplitude threshold $\varsigma_p = -20$ dB. Therefore, we can conclude that the presented antenna placement technique also yields fairly accurate results in realistic operative scenarios. However, we stress that rigorous modeling of mutual coupling in sparse arrays is not trivial and strongly

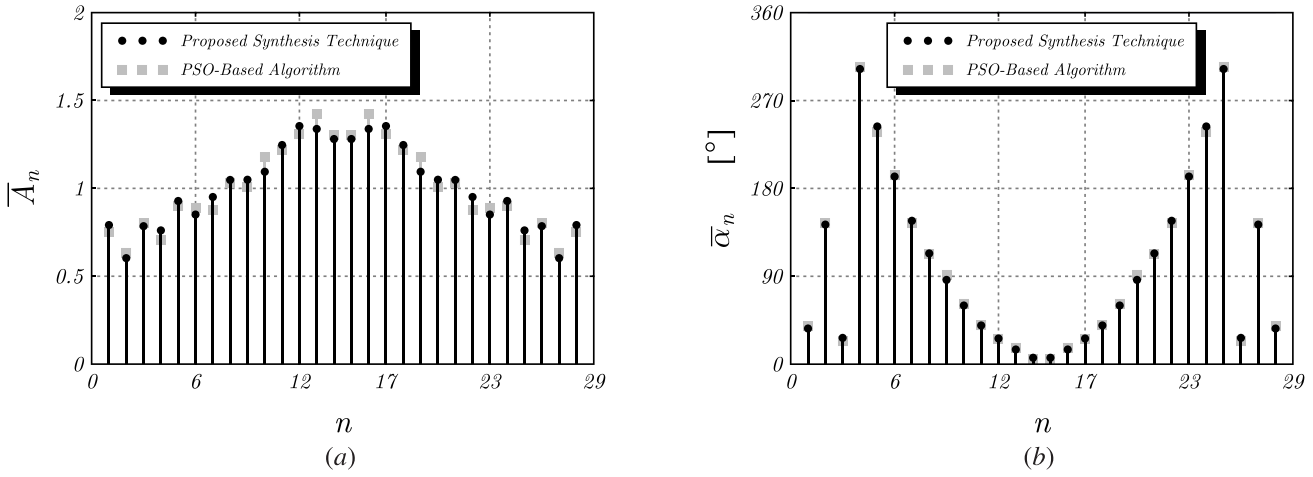

Fig. 5. (a) Magnitude and (b) phase of the excitation coefficients of a sparse arc array of aperture $L_a = 24\,\lambda_0$ and curvature radius $R_a = 30\,\lambda_0$ consisting of $N_a = 28$ uniform antenna elements that synthesizes a pencil-beam radiation pattern with HPBW $\Theta_0 = 6°$ and PSL $\varsigma_p = -20$ dB.

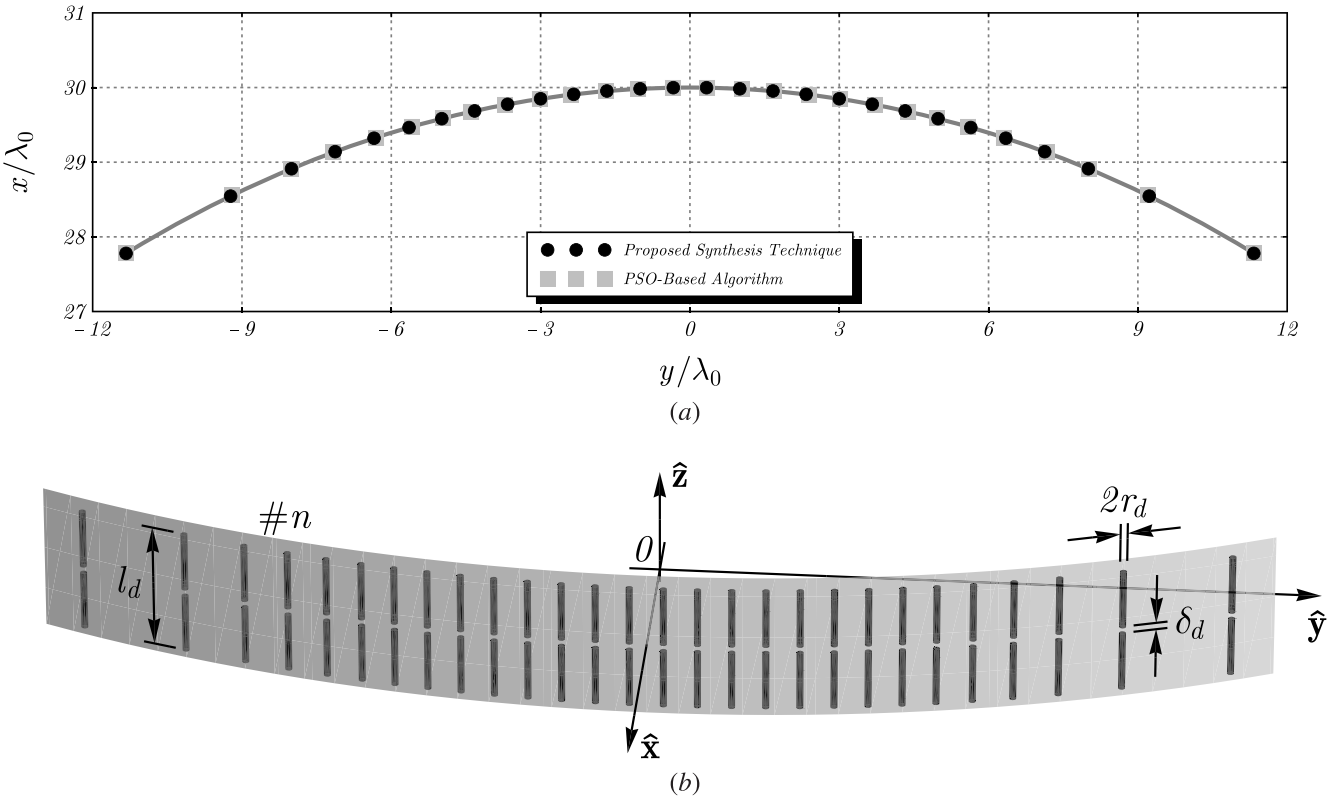

Fig. 6. (a) Antenna element positions and (b) dipole-based implementation of a sparse arc array with aperture $L_a = 24\,\lambda_0$ and curvature radius $R_a = 30\,\lambda_0$ featuring a pencil-beam radiation pattern with HPBW $\Theta_0 = 6°$ and PSL $\varsigma_p = -20$ dB. The number of array elements embedded in the radiating structure is $N_a = 28$. Each dipole antenna is characterized by length $l_d = 0.425\,\lambda_0$, radius $r_d = 0.0125\,\lambda_0$, and feeding delta gap $\delta_d = 0.005\,\lambda_0$.

problem dependent. In designs that are adversely challenged by poor antenna isolation and/or characterized by a large number of radiating elements embedded in the array structure, the developed algorithm might be adopted as an effective preconditioner in hybrid deterministic/metaheuristic synthesis methodologies in order to derive a well-conditioned initial array configuration for enhancing convergence in terms of a number of iterations within the metaheuristic procedure and consequently reducing the total computational time required to obtain a converged solution of the problem [45].

By keeping the array aperture size $L_a = 24\,\lambda_0$ and number of antennas $N_a = 28$ unchanged, a parameter study has been performed to determine the PSL ς_p achieved in combination with the targeted HPBW $\Theta_0 = 6°$ as a function of the minimum separation $\Delta s_{\min}$ enforced between the radiating elements. The outcome of the analysis is shown in Fig. 10 where one can notice that the design specification $\varsigma_p \leqslant -20$ dB is successfully met for $0.64 \lesssim \Delta s_{\min}/\lambda_0 \lesssim 0.8$ with the array sparsity ratio $\Delta s_{\max}/\Delta s_{\min}$ between the maximum and minimum interelement spacings ranging from about 3.725 down to 1.745. It is worth pointing out that as the antenna placement tends to become more uniform ($\Delta s_{\max}/\Delta s_{\min} \to 1^-$), a progressive performance degradation in terms of PSL is noticed, showing, in the

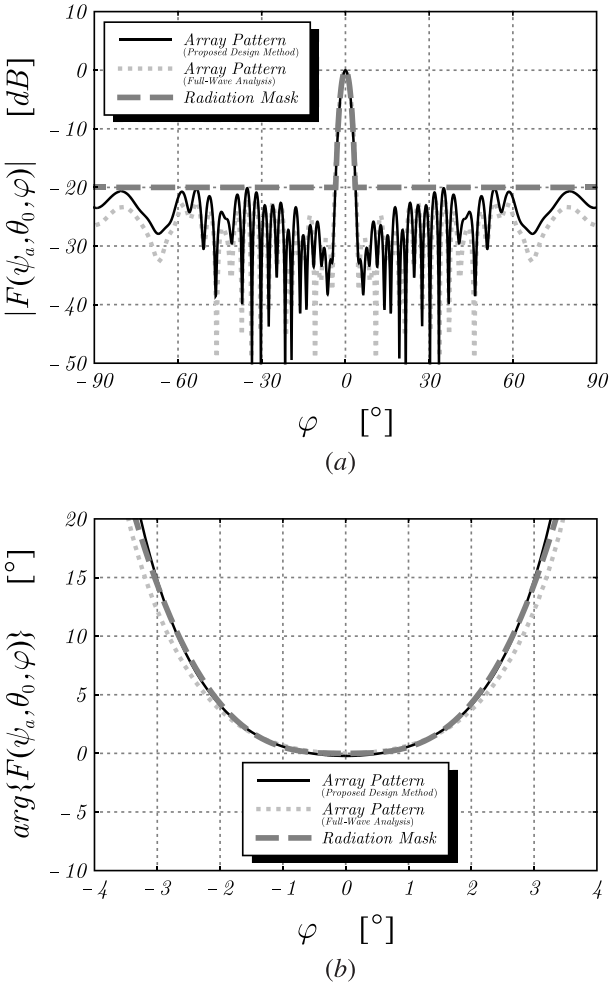

Fig. 7. (a) Magnitude and (b) phase of the synthesized radiation pattern of a sparse arc array of aperture $L_a = 24\,\lambda_0$ and curvature radius $R_a = 30\,\lambda_0$ consisting of $N_a = 28$ uniformly radiating elements with minimal separation $d_{\min} \geqslant 2\,\lambda_0/3$.

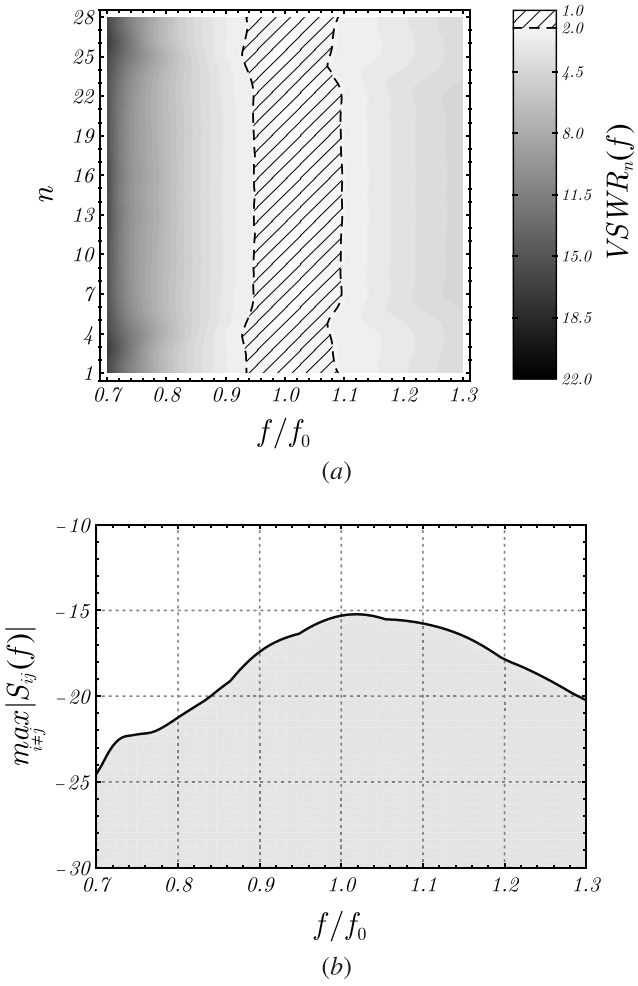

Fig. 8. (a) Frequency-domain behavior of embedded VSWR and (b) maximum coupling level featured by the dipole antenna elements of the aperiodic array shown in Fig. 6(b).

specific considered example, the benefits of an aperiodic array architecture.

4) Computational Complexity Analysis: The example described in this section illustrates the versatility of the developed technique, which provides antenna engineers with an effective array synthesis tool that allows for a combined controllable tapering of the illumination distribution and element density and, hence, yields a number of useful degrees of freedom in constrained design problems for a great variety of applications with different requirements for antenna spacing, number of radiating elements, and array sparseness characteristics (uniform/aperiodic placement). An additional favorable feature of the considered methodology lies in the relevant fully deterministic formulation, which typically results in reduced computational times and negligible memory usage compared with evolutionary stochastic methods for which the complexity increases dramatically (at exponential rate) with the number of problem unknowns as per the Nemirovsky–Yudin theorem [46]. In order to point out this important aspect, the problem of synthesizing a circular arc sparse array featuring a pencil-beam radiation pattern with the aforementioned characteristics (see Fig. 7) has been addressed, also, by means of an evolutionary procedure based on a particle swarm optimization (PSO) algorithm [47]. In doing so, all the numerical computations have been performed in double-precision floating-point arithmetic on the same computer equipped with a 2.2 GHz Intel Core i7 processor [48] and 16 GB random access memory (RAM). Notably, the considered approaches yield pretty similar results in terms of antenna positions and excitation coefficients [see Figs. 5 and 6] although, as it can be noticed in Table I, the presented analytical synthesis technique, enabling nearly real-time computing capability, outperforms the alternative stochastic methodology.

B. Constrained Design of a Conformal Isoflux Antenna Array

1) Design Problem: In this section, the effectiveness of the proposed antenna placement technique is verified by application to the design of an array featuring shaped radiation pattern characteristics for synthetic aperture radar (SAR) [49], [50]. As know from literature [51], SAR systems rely on Doppler signal processing for the retrieval of high-resolution images in the azimuth direction [see Fig. 11(a)]. To operate such a system in the wide-scan mode, an array antenna with a flat phase front over a broad angular range is needed. To this end, the synthesis on an isoflux beam [as shown in Fig. 11(b)]

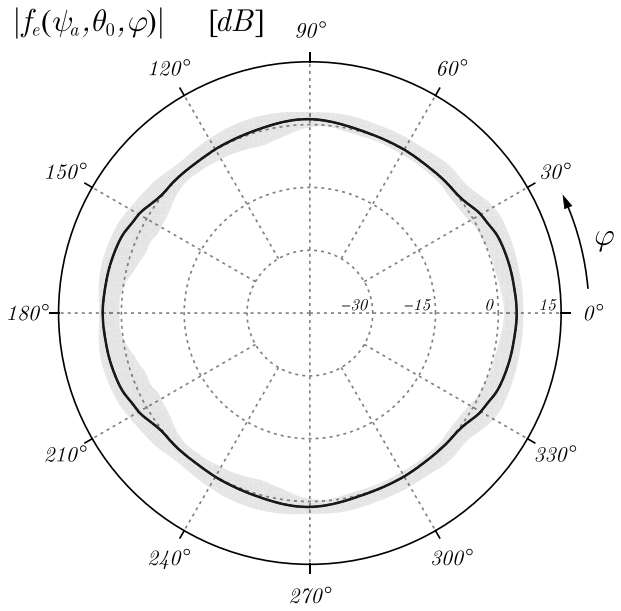

Fig. 9. Angular distribution of the average AEP displayed by the dipole antennas forming the nonuniformly spaced array shown in Fig. 6(b) at the central working frequency $f = f_0$ along the azimuthal observation plane $\vartheta = \theta_0 = \pi/2$. Shaded area graphically denotes the range variability of the AEP across the various antenna elements.

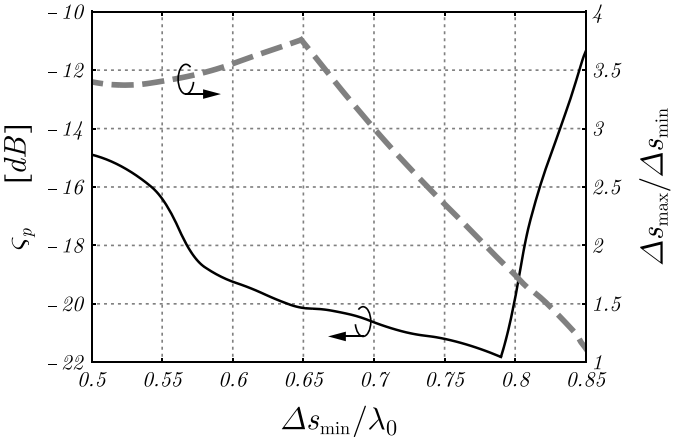

Fig. 10. PSL ς_p and sparsity ratio $\Delta s_{\max}/\Delta s_{\min}$ of a pencil-beam arc array of aperture $L_a = 24\,\lambda_0$ and curvature radius $R_a = 30\,\lambda_0$ consisting of $N_a = 28$ uniform antenna elements with minimum interelement spacing $\Delta s_{\min}$.

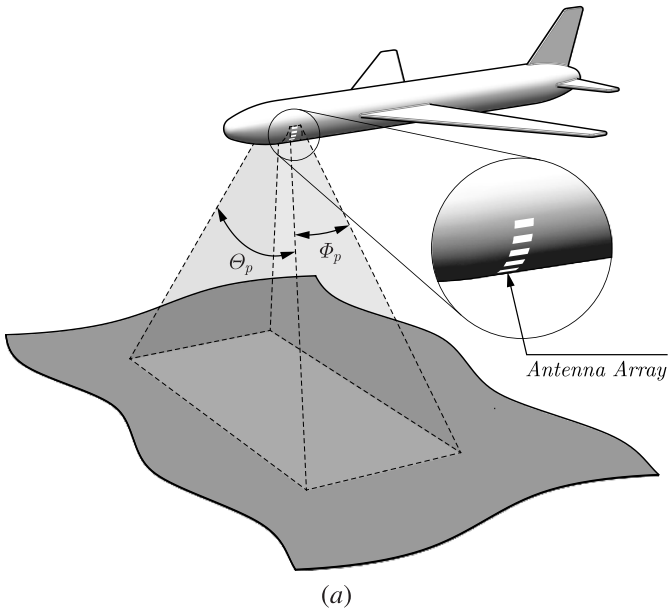

(a)

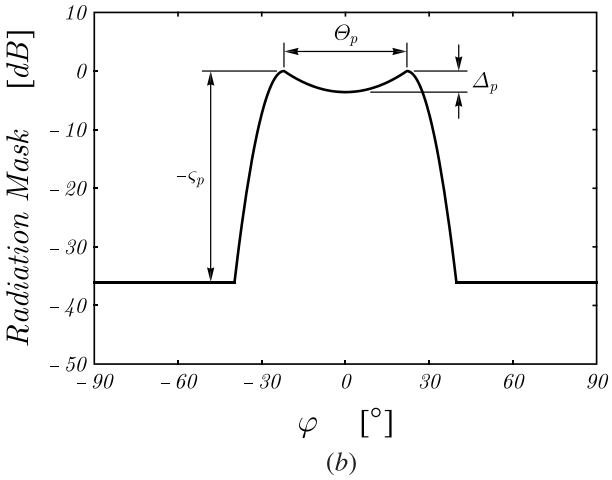

(b)

Fig. 11. (a) Conformal antenna array for SAR surveys and (b) relevant radiation pattern mask for isoflux illumination of the target.

is beneficial for achieving optimal uniform coverage of the target while maximizing radar performance in terms of equivalent isotropically radiated power (EIRP) [52] and radiometric accuracy.

We consider the problem of synthesizing a conformal array that matches the radiation mask plotted in Fig. 11(b) under the hypothesis that the beam plateau region is characterized by a swath angle $\Theta_p = 28°$ and dynamic amplitude range $\Delta_p = 3$ dB while enforcing the PSL to be $\varsigma_p = -20$ dB in combination with a flat phase distribution $\arg\{F_O(\varphi)\} = 0$ along the entire plateau range [31]. Furthermore, we assume that the individual antenna element embedded in the array features the radiation pattern $f(\psi_a, \theta_0, \varphi) \propto \cos\varphi$ along the observation plane $\vartheta = \theta_0 = \pi/2$. In this case, the normalized elementary radiated field contribution from the general mth subdomain of the array is given by

$$\begin{aligned}\Delta E_m(\psi_a, \vartheta, \varphi) &= -\frac{j}{\pi}\frac{\partial}{\partial \psi_a}\int_{\varphi-\upsilon_m}^{\varphi-\upsilon_{m-1}} e^{j\psi_a \cos w} dw \\ &= j\frac{\partial}{\partial \psi_a}\left[\mathbf{A}_0\left(\frac{\pi}{2} - \upsilon_m + \varphi, \psi_a\right)\right. \\ &\qquad \left. - \mathbf{A}_0\left(\frac{\pi}{2} - \upsilon_{m-1} + \varphi, \psi_a\right)\right] \qquad (3)\end{aligned}$$

where the first derivative of the incomplete Anger–Weber functions can be evaluated using the relevant recurrence formulas in combination with the relevant asymptotic expansions [53]. By applying the point-matching procedure described in [28, Sec. II-B], the complex array illumination $\gamma(\upsilon)$, which is useful for synthesizing the considered radiation pattern mask (see Fig. 12), can be readily determined.

2) Synthesis Neglecting Antenna Coupling: Under the assumption that the radiating structure is integrated on a circular platform with normalized radius $R_a/\lambda_0 = 21$ while enforcing a minimum antenna separation $d_{\min} = 11\,\lambda_0/20$,

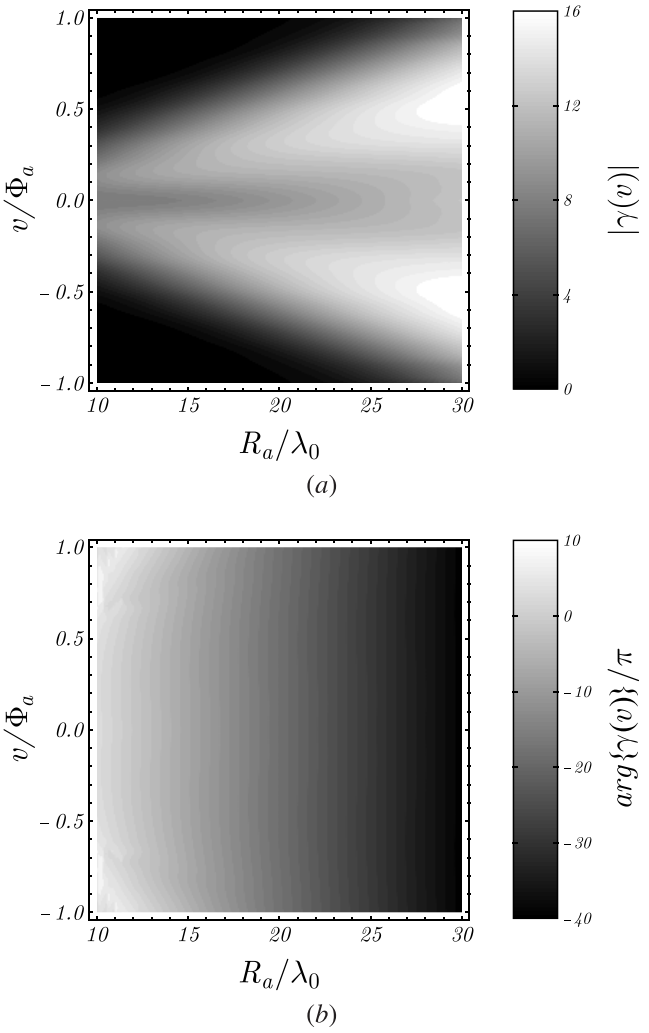

Fig. 12. (a) Magnitude and (b) phase of the taper distribution $\gamma\ (v)$ relevant to an isoflux conformal array of aperture $L_a = 23\,\lambda_0$ as a function of the normalized radius R_a/λ_0 of the circular platform on which the radiating structure is integrated.

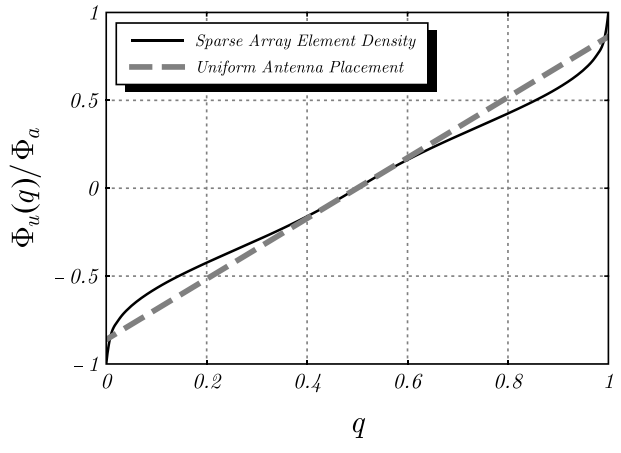

Fig. 13. Angular element density relevant to an isoflux conformal array with aperture $L_a = 23\,\lambda_0$ and curvature radius $R_a = 21\,\lambda_0$ subject to the design constraint on minimum antenna separation $d_{\min} = 11\,\lambda_0/20$.

the angular element density function $\Phi_u(q)$ is found to exhibit the distribution shown in Fig. 13. The relevant continuous excitation amplitude and phase of the considered array can

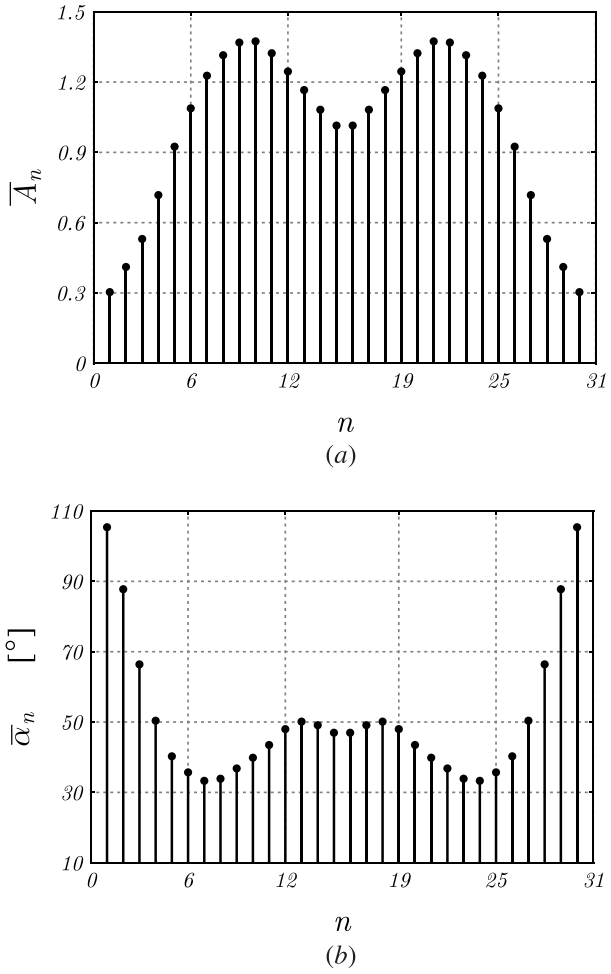

Fig. 14. (a) Magnitude and (b) phase of the excitation coefficients of a conformal array with aperture $L_a = 23\,\lambda_0$ and curvature radius $R_a = 21\,\lambda_0$ consisting of $N_a = 30$ antenna elements that synthesize an isoflux radiation pattern with HPBW $\Theta_p = 28°$, PSL $\varsigma_p = -20$ dB, and dynamic amplitude range $\Delta_p = 3$ dB along the swath angle of the main beam.

be computed as follows:

$$A_u(q) = \frac{1}{\pi}\left|\gamma\left(\Phi_u(q)\right)\right|\Phi_u'(q) \tag{4}$$

and

$$\alpha_u(q) = \arg\left\{\gamma\left(\Phi_u(q)\right)\right\}, \tag{5}$$

respectively.

Using the Nyquist-theorem-based criterion detailed in [28], it can be found out that the optimal number of discrete antenna elements to be integrated along the array aperture is $N_a = 30$. The resulting antenna excitation coefficients obtained by sampling of the functions in (4) and (5) are shown in Fig. 14, and the schematic of the array topology is shown in Fig. 15(a). The minimum and maximum interelement spacings are $0.69\,\lambda_0$ ($> d_{\min}$) and $0.96\,\lambda_0$, respectively, with an average antenna separation of approximately $0.79\,\lambda_0$. As shown in Fig. 16, both magnitude and phase of the synthesized pattern match well the assigned radiation mask.

3) Synthesis Considering Antenna Coupling: To assess the impact of parasitic electromagnetic coupling, the considered

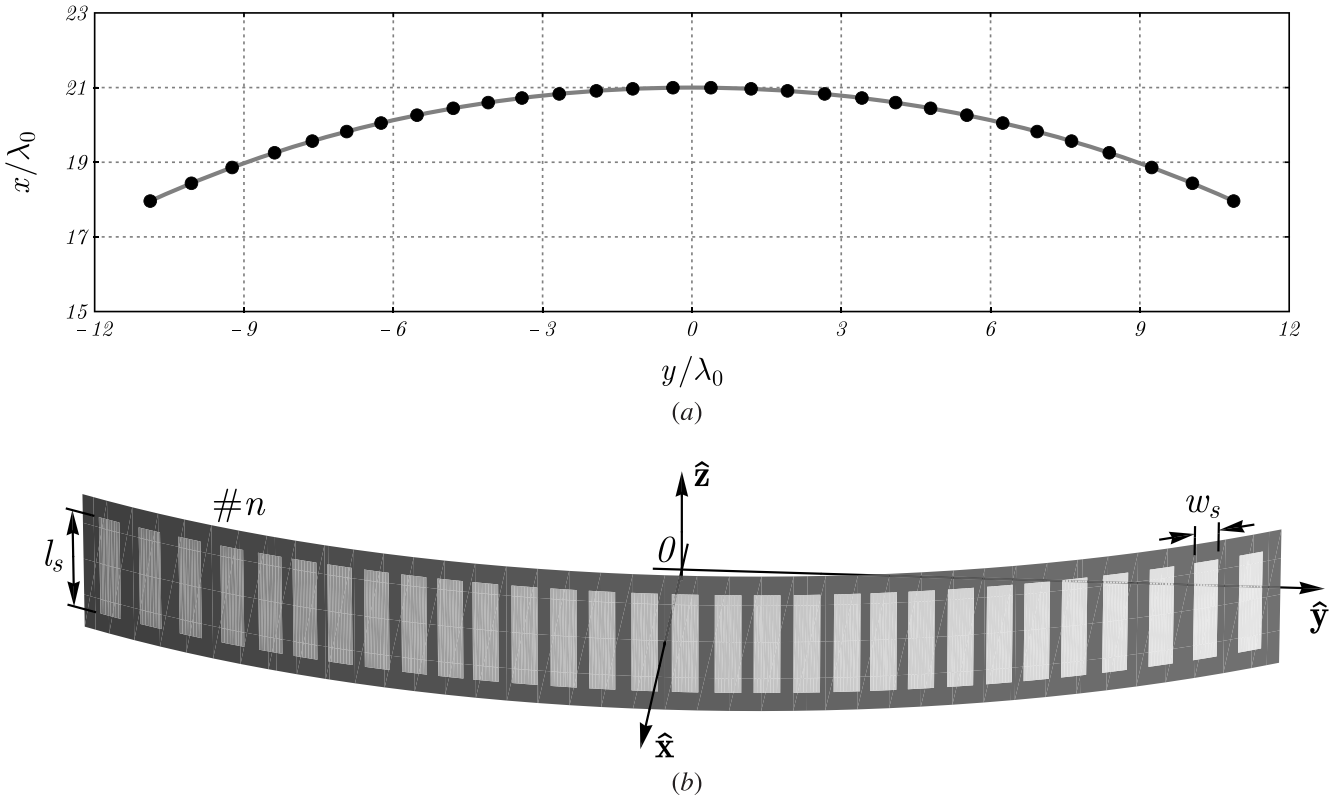

Fig. 15. (a) Element positions and (b) pictorial sketch of the slot-based antenna implementation of a conformal array with aperture $L_a = 23\,\lambda_0$ and curvature radius $R_a = 21\,\lambda_0$ featuring an isoflux radiation pattern. The number of array elements embedded in the radiating structure is $N_a = 30$. Each slot antenna is characterized by length $l_s = 0.607\lambda_0$ and width $w_s = 0.0367\lambda_0$ which are selected in such a way as to ensure optimal performance at the working frequency $f_0 = c_0/\lambda_0$.

array architecture was implemented using slot antenna technology [54]. A pictorial sketch (not to scale) of the structure is shown in Fig. 15(b). The individual antenna element, with length $l_s = 0.607\,\lambda_0$ and width $w_s = 0.0367\,\lambda_0$, is directly fed by a coaxial cable with characteristic impedance $Z_0 = 50\ \Omega$ soldered across the middle section of the radiating aperture. The various slots, whose placement follows the angular distribution in Fig. 15(a), are assumed to be realized by photolithographic etching of a single-layer grounded dielectric slab with linear dimensions $l_g = 24.5\,\lambda_0$, $h_g = \lambda_0$, thickness $t_d = 0.002\,\lambda_0$, and relative permittivity $\varepsilon_r = 4.3$. The full-wave characterization of the array was conducted using the locally conformal FDTD technique in [42] and [43], revealing that the considered design features very good performance in terms of embedded voltage standing wave ratio (VSWR), namely, $\mathrm{VSWR}_n \lesssim 1.11 : 1$ (with $i = 1, 2, \ldots, N_a$) at the central working frequency $f_0 = c_0/\lambda_0$. Furthermore, the minimum isolation level between the radiating elements was found to be $I_{\min}(f_0) = -20 \log \max_{i \neq j} |S_{ij}(f_0)| \simeq 16.0$ dB [31].

The parasitic antenna coupling is responsible for a nonmarginal deviation of the average AEP (not shown here for the sake of shortness) from the nominal pattern $f(\psi_a, \theta_0, \varphi) \propto \cos\varphi$ [31], resulting in a slight degradation of the phase of the AAP in the neighborhood of the boresight $\varphi = 0°$ [see Fig. 16(b)]. Conversely, a visual inspection of Fig. 16(a) indicates that the magnitude of the AAP shows a reduced sensitivity to the aforementioned antenna nonideality such that an overall satisfactory consistency with the assigned radiation mask is preserved. By using the synthesis procedure described in [28], the amplitude tapering of the considered array design [see Fig. 14(a)] can be easily quantized in such a way that only a finite number N_p of power levels are operated within the beam-forming network of the radiating structure. Such a design constraint requires a suitable perturbation of the antenna placement as described next. Let us consider the specific case where $N_p = 4$, assuming that 2-bit digitally controlled programmable gain amplifiers (PGAs) [55] are integrated in the radio-frequency (RF) chain of the system to control and taper the radiation pattern of the array. The constrained illumination amplitude $A_c(q)$ resulting from the power level quantization can be readily evaluated by the application of [28, eq. (27)] to the unconstrained distribution $A_u(q)$. As such, the perturbed element density function $\Phi_c(q)$ follows from the numerical solution for $-\Phi_a \leqslant v \leqslant \Phi_a$ of the following integral equation:

$$\frac{\int_0^{\Phi_c^{-1}(v)} A_c(w)\,dw}{\int_0^{\Phi_u^{-1}(v)} A_u(w)\,dw} = 1 \tag{6}$$

and the subsequent inversion by Lagrange interpolation. The constrained illumination phase is then derived as follows:

$$\alpha_c(q) = \arg\{\gamma(\Phi_c(q))\}. \tag{7}$$

The antenna excitation coefficients, which were obtained by indicial sampling of $A_c(q)$ and $\alpha_c(q)$ while holding the number of radiating elements unchanged ($N_a = 30$), are

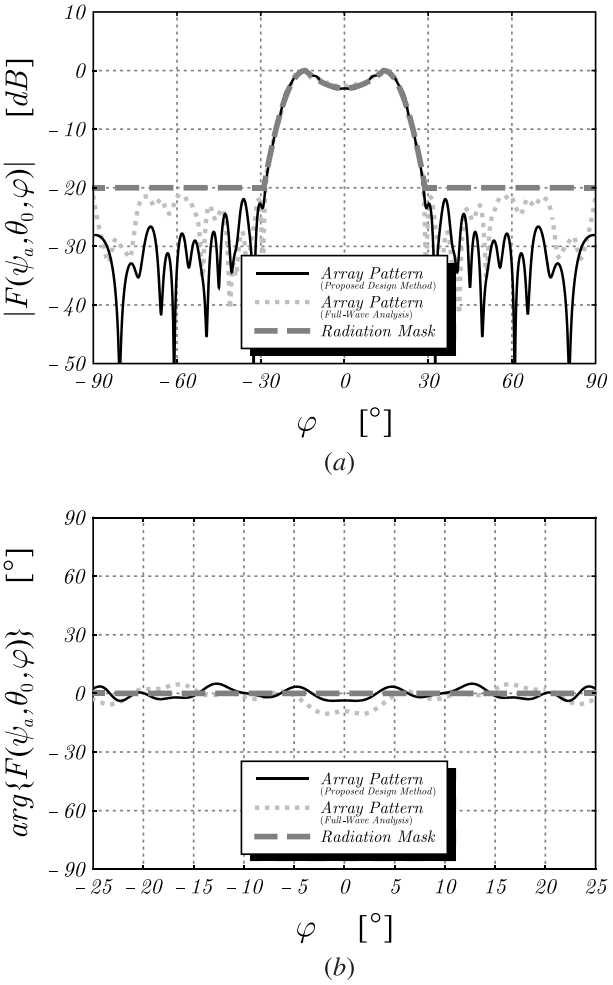

Fig. 16. (a) Magnitude and (b) phase of the isoflux radiation pattern of a conformal array with aperture $L_a = 23\,\lambda_0$ and curvature radius $R_a = 21\,\lambda_0$ consisting of $N_a = 30$ antenna elements, as shown in Fig. 15.

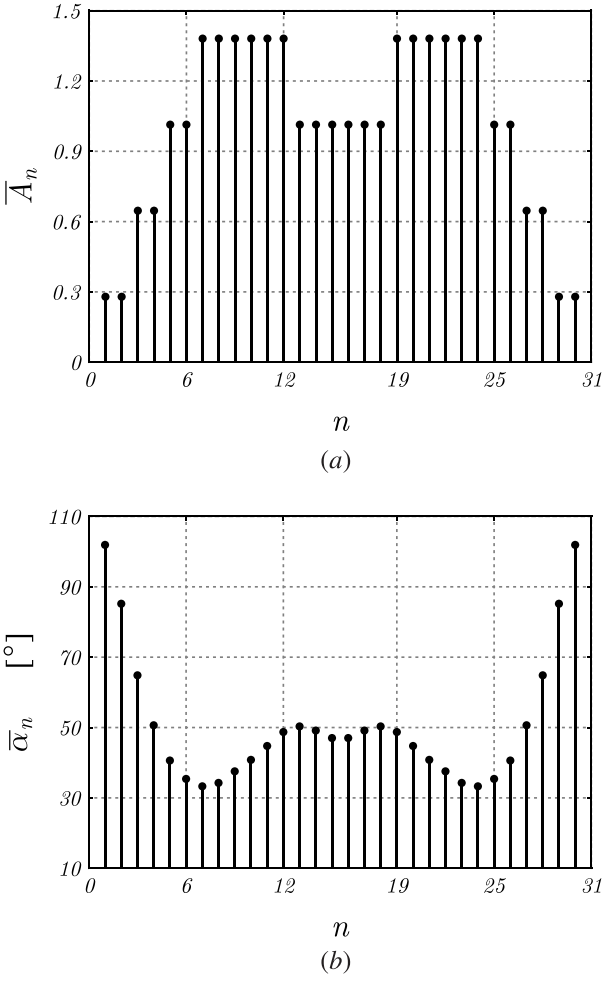

Fig. 17. (a) Magnitude and (b) phase of the excitation coefficients of a conformal array with aperture $L_a = 23\,\lambda_0$ and curvature radius $R_a = 21\,\lambda_0$, consisting of $N_a = 30$ antenna elements that synthesize an isoflux radiation pattern subject to the design constraint on the maximum number of power levels ($N_p = 4$) to be operated in the beam-forming network of the radiating structure.

shown in Fig. 17, and the optimized array topology is shown in Fig. 18(a). The minimum interelement spacing was found to be $0.56\,\lambda_0$, which is consistent with the design constraint on antenna placement, whereas the average separation between the adjacent radiating elements is approximately $0.77\,\lambda_0$. In the considered example, the quantization of the excitation amplitude tapering has resulted in a higher degree of sparsity in the structure. As shown in Fig. 18, the synthesized pattern matches the prescribed radiation mask in a satisfactory manner.

4) Experimental Validation: The constrained array architecture was physically implemented using slot antenna technology. The same guidelines illustrated in relation to the unconstrained design [see Fig. 15(b)] were adopted. In particular, the structure has been realized in such a way as to display a central resonant frequency $f_0 = 5$ GHz. To this end, a grounded FR4 laminate with thickness $t_d = 0.125$ mm, relative permittivity $\varepsilon_r \simeq 4.36$, and loss tangent $\tan\delta \simeq 0.016$ at frequency $f = 1$ GHz was used as an antenna substrate. The radiating slots etched on the substrate feature the linear dimensions of $l_s = 3.64$ cm and $w_s = 2.2$ mm and are fed by 20 cm-long shielded coaxial cables with subminiature version A (SMA) connectors. As shown in Fig. 19(a), the antenna elements are distributed along the array aperture (with length $l_g = 1.465$ m and height $h_g = 6$ cm) according to the schematic in Fig. 18(a). A custom conformal platform composed of foam is used as a physical support with the desired curvature radius $R_a \simeq 1.25$ m.

The scattering parameter measurements taken on the physical prototype were used to verify that $VSWR_n\,(f_0) \lesssim 1.75 : 1$ for $i = 1, 2, \ldots, N_a$ and the minimum isolation between the antennas is approximately 16.2 dB, including the losses of the feeding cables. The relevant results are not shown here for the sake of brevity. The radiation properties of the structure were characterized in a fully anechoic chamber [see Fig. 19(b)]. The various antenna elements were fed individually in such a way as to evaluate the relevant AEPs. In this way, the array radiation pattern could be evaluated by off-line postprocessing and is shown in Fig. 18. One can notice a good consistency with the reference isoflux mask, although parasitics that are neglected in the synthesis model and, more importantly, manufacturing tolerances are responsible for the excitation of a spurious radiation lobe along the angular direction $\varphi \simeq 37.5°$ [see Fig. 18(b)].

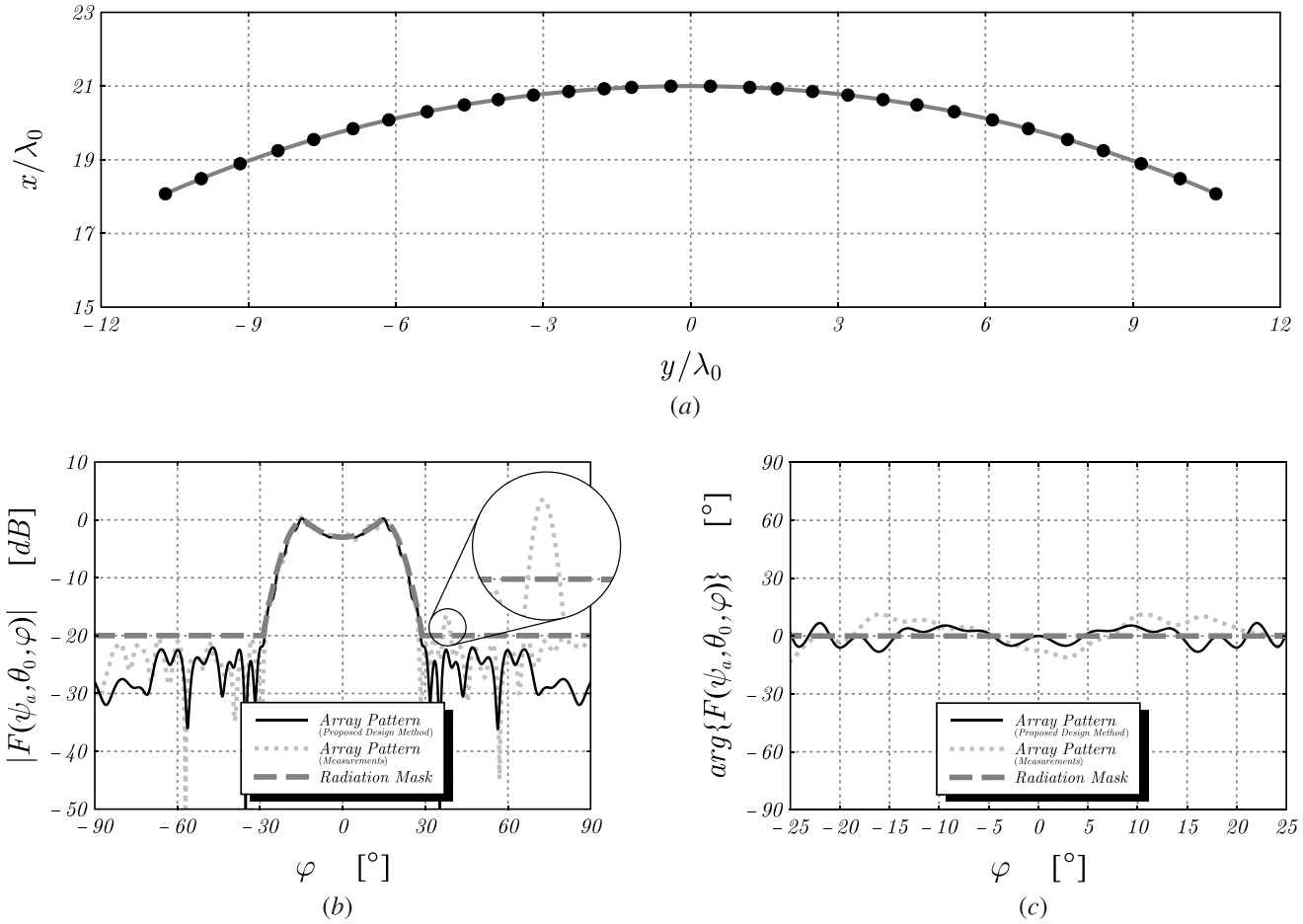

Fig. 18. (a) Antenna placement and (b) magnitude and (c) phase of the radiation pattern synthesized by a conformal array consisting of $N_a = 30$ antenna elements whose excitation is constrained in such a way as to feature a finite number ($N_p = 4$) of power levels, as shown in Fig. 17.

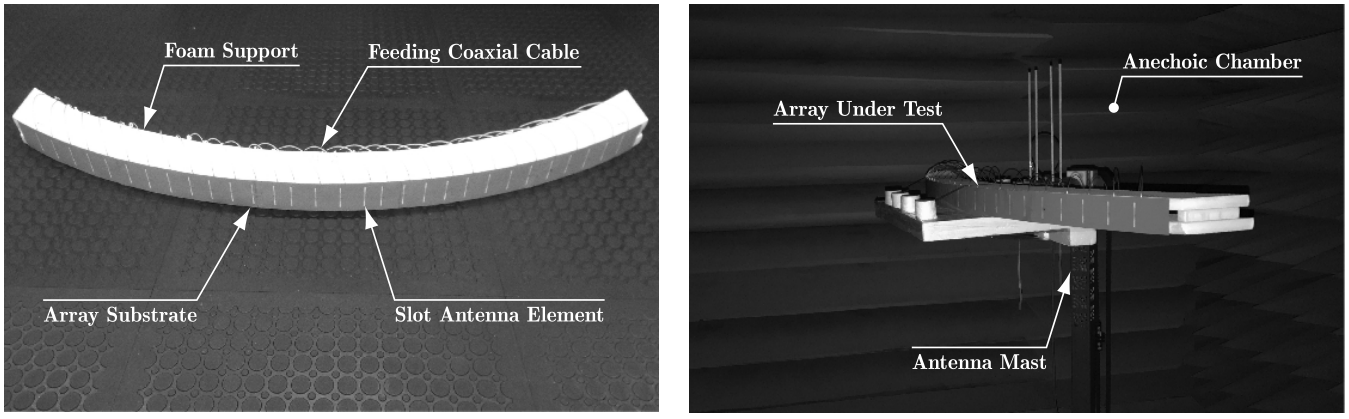

Fig. 19. (a) Physical prototype of an aperiodic conformal antenna array consisting of $N_a = 30$ slot antennas that synthesize an isoflux radiation pattern, subject to design constraints on the minimum interelement spacing, and a maximum number of power levels to be operated in the feeding network of the radiating structure. (b) Measurement setup for the characterization of the array radiation properties in a fully anechoic chamber.

III. Conclusion

A general and effective deterministic antenna placement methodology for aperiodic conformal arrays has been presented. By using the proposed procedure, complex array synthesis problems subject to demanding requirements in terms of the maximum aperture size, minimum interelement spacing, or maximum number of power levels to be operated in the beam-forming network can be addressed in a straightforward and computationally inexpensive manner.

The developed technique has been successfully assessed and validated by application to the synthesis of antenna arrays featuring pencil-beam or shaped radiation pattern masks typically

adopted in satellite communications and radar applications. The impact of parasitic antenna coupling has been investigated by performing dedicated full-wave analyses and experimental measurements. The obtained results showed that the presented design methodology yields reasonably accurate results even in operative scenarios in which a significant deviation from ideal antenna operation occurs.

ACKNOWLEDGMENT

The authors would like to thank J. Sofalvi for the help in the graphical presentation of the results.

REFERENCES

[1] A. J. Fenn, D. H. Temme, W. P. Delaney, and W. E. Courtney, "The development of phased-array radar technology," *Lincoln Lab. J.*, vol. 12, no. 2, pp. 321–340, 2000.

[2] T. E. Morton and K. M. Pasala, "Pattern synthesis of conformal arrays for airborne vehicles," in *Proc. IEEE Aerosp. Conf. Proc.*, Big Sky, MT, USA, Mar. 2004, pp. 1030–1038.

[3] W. A. Imbriale, S. Gao, and L. Boccia, *Space Antenna Handbook*. Hoboken, NJ, USA: Wiley, 2012.

[4] B. P. Kumar and G. R. Branner, "Generalized analytical technique for the synthesis of unequally spaced arrays with linear, planar, cylindrical or spherical geometry," *IEEE Trans. Antennas Propag.*, vol. 53, no. 2, pp. 621–634, Feb. 2005.

[5] *Innovative Architectures for Reducing the Number of Controls of Multiple Beam Telecommunications Antennas*, document ESA/ESTEC Tender AO/1-5598/08/NL/ST, Jan. 2008.

[6] M. C. Viganó, G. Toso, P. Angeletti, I. E. Lager, A. Yarovoy, and D. Caratelli, "Sparse antenna array for Earth-coverage satellite applications," in *Proc. 4th Eur. Conf. Antennas Propag.*, Apr. 2010, pp. 1–4.

[7] M. C. Viganó and D. Caratelli, "Analytical synthesis technique for uniform-amplitude linear sparse arrays," in *Proc. IEEE Antennas Propag. Soc. Int. Symp.*, Jul. 2010, pp. 1–4.

[8] D. Caratelli, M. C. Viganó, G. Toso, and P. Angeletti, "Analytical placement technique for sparse arrays," in *Proc. 32nd ESA Antenna Workshop*, Oct. 2010, pp. 5–8.

[9] D. Caratelli and M. C. Viganó, "Analytical synthesis technique for linear uniform-amplitude sparse arrays," *Radio Sci.*, vol. 46, no. 4, pp. 1–6, Aug. 2011.

[10] D. Caratelli and M. C. Viganó, "A novel deterministic synthesis technique for constrained sparse array design problems," *IEEE Trans. Antennas Propag.*, vol. 59, no. 11, pp. 4085–4093, Nov. 2011.

[11] P. Angeletti and G. Toso, "Array antennas with jointly optimized elements positions and dimensions part I: Linear arrays," *IEEE Trans. Antennas Propag.*, vol. 62, no. 4, pp. 1619–1626, Apr. 2014.

[12] P. Angeletti, G. Toso, and G. Ruggerini, "Array antennas with jointly optimized elements positions and dimensions part II: Planar circular arrays," *IEEE Trans. Antennas Propag.*, vol. 62, no. 4, pp. 1627–1639, Apr. 2014.

[13] L. Josefsson and P. Persson, *Conformal Array Antenna Theory Design*. Hoboken, NJ, USA: Wiley, 2006.

[14] D. Caratelli, I. Liberal, and A. Yarovoy, "Design and full-wave analysis of conformal ultra-wideband radio direction finders," *IET Microw., Antennas Propag.*, vol. 5, no. 10, pp. 1164–1174, Jul. 2011.

[15] A. F. Peterson, S. L. Ray, and R. Mittra, *Computational Methods for Electromagnetics*. Hoboken, NJ, USA: Wiley, 1997.

[16] D. B. Davidson, *Computational Electromagnetics for RF and Microwave Engineering*. Cambridge, U.K.: University Press, 2010.

[17] A. Akhmanov and S. Y. Nikitin, *Physical Optics*. New York, NY, USA: Oxford University Press, 1997.

[18] D. A. McNamara, C. W. I. Pistorius, and J. A. G. Malherbe, *Introduction to Uniform Geometrical Theory Diffraction*. Boston, MA, USA:: Artech House, 1990.

[19] H. Lebret and S. Boyd, "Antenna array pattern synthesis via convex optimization," *IEEE Trans. Signal Process.*, vol. 45, no. 3, pp. 526–532, Mar. 1997.

[20] F. J. Ares-Pena, J. A. Rodriguez-Gonzalez, E. Villanueva-Lopez, and S. R. Rengarajan, "Genetic algorithms in the design and optimization of antenna array patterns," *IEEE Trans. Antennas Propag.*, vol. 47, no. 3, pp. 506–510, Mar. 1999.

[21] T. Girard, R. Staraj, E. Cambiaggio, and F. Müller, "A simulated annealing algorithm for planar or conformal antenna array synthesis with optimized polarization," *Microw. Opt. Technol. Lett.*, vol. 28, no. 2, pp. 86–89, Jan. 2001.

[22] K. Chen, X. Yun, Z. He, and C. Han, "Synthesis of sparse planar arrays using modified real genetic algorithm," *IEEE Trans. Antennas Propag.*, vol. 55, no. 4, pp. 1067–1073, Apr. 2007.

[23] W. T. Li, X. W. Shi, Y. Q. Hei, S. F. Liu, and J. Zhu, "A hybrid optimization algorithm and its application for conformal array pattern synthesis," *IEEE Trans. Antennas Propag.*, vol. 58, no. 10, pp. 3401–3406, Oct. 2010.

[24] R. Bhattacharya, T. K. Bhattacharyya, and R. Garg, "Position mutated hierarchical particle swarm optimization and its application in synthesis of unequally spaced antenna arrays," *IEEE Trans. Antennas Propag.*, vol. 60, no. 7, pp. 3174–3181, Jul. 2012.

[25] X. Li, W.-T. Li, X.-W. Shi, and J. Yang, "Synthesis of antenna arrays with an efficient multiobjective differential evolution algorithm," *Int. J. RF Microw. Comput.-Aided Eng.*, vol. 24, no. 2, pp. 161–169, Mar. 2014.

[26] D. Caratelli and M. C. Viganó, "Analytical synthesis technique for linear uniform-amplitude sparse arrays," *Radio Sci.*, vol. 46, no. 4, pp. 1–6, Aug. 2011.

[27] D. Caratelli, M. C. Viganó, and A. Yarovoy, "Deterministic synthesis of non-uniformly spaced isophoric linear antenna arrays," in *Proc. Int. Symp. Electromagn. Theory*, May 2013, pp. 602–605.

[28] D. Caratelli, G. Toso, O. V. Stukach, and N. V. Panokin, "Deterministic constrained synthesis technique for conformal aperiodic linear antenna arrays—Part I: Theory," *IEEE Trans. Antennas Propag.*, vol. 67, no. 9, pp. 5951–5961, Sep. 2019.

[29] D. Caratelli, G. Toso, and P. Angeletti, "On the deterministic synthesis of aperiodic ring antenna arrays," in *Proc. 8th Eur. Conf. Antennas Propag.*, Apr. 2014, pp. 1250–1254.

[30] D. Caratelli and G. Toso, "Deterministic synthesis of conformal linear aperiodic antenna arrays," in *Proc. IEEE Int. Symp. Antennas Propag.*, Jul. 2017, pp. 2015–2016.

[31] D. Caratelli and G. Toso, "Deterministic synthesis of complex shaped-beam radiation patterns using conformal aperiodic antenna arrays," in *Proc. 12th Eur. Conf. Antennas Propag.*, Apr. 2018, pp. 1–5.

[32] A. Oliner and G. Knittel, "Mutual coupling effects in circular arrays on cylindrical surfaces—Aperture design implications and analysis," in *Phased Array Antennas*. Dedham: Artech House, 1972.

[33] Q. Balzano and T. Dowling, "Mutual coupling analysis of arrays of apertures on cones," *IEEE Trans. Antennas Propag.*, vol. 22, no. 1, pp. 92–97, Jan. 1974.

[34] S. Raffaelli, Z. Sipus, and P. S. Kildal, "Analysis and measurements of conformal patch array antennas on multilayer circular cylinder," *IEEE Trans. Antennas Propag.*, vol. 53, no. 3, pp. 1105–1113, Mar. 2005.

[35] A. Lay-Ekuakille, P. Vergallo, N. I. Giannoccaro, A. Massaro, and D. Caratelli, "Prediction and validation of outcomes from air monitoring sensors and networks of sensors," in *Proc. 5th Int. Conf. Sens. Technol.*, Dec. 2011, pp. 73–78.

[36] V. B. Erturk, R. G. Rojas, and K. W. Lee, "Analysis of finite arrays of axially directed printed dipoles on electrically large circular cylinders," *IEEE Trans. Antennas Propag.*, vol. 52, no. 10, pp. 2586–2595, Oct. 2004.

[37] Q. Yuan, Q. Chen, and K. Sawaya, "Performance of adaptive array antenna with arbitrary geometry in the presence of mutual coupling," *IEEE Trans. Antennas Propag.*, vol. 54, no. 7, pp. 1991–1996, Jul. 2006.

[38] D. M. Pozar, "The active element pattern," *IEEE Trans. Antennas Propag.*, vol. 42, no. 8, pp. 1176–1178, Sep. 1994.

[39] D. M. Pozar, "A relation between the active input impedance and the active element pattern of a phased array," *IEEE Trans. Antennas Propag.*, vol. 51, no. 9, pp. 2486–2489, Sep. 2003.

[40] C. A. Balanis, *Antenna Theory: Analysis and Design*. Hoboken, NJ, USA: Wiley, 2016.

[41] C. L. Dolph, "A current distribution for broadside arrays which optimizes the relationship between beam width and side-lobe level," *Proc. IRE*, vol. 34, no. 6, pp. 335–348, Jun. 1946.

[42] D. Caratelli, A. Massaro, R. Cingolani, and A. G. Yarovoy, "Accurate time-domain modeling of reconfigurable antenna sensors for non-invasive melanoma skin cancer detection," *IEEE Sensors J.*, vol. 12, no. 3, pp. 635–643, Mar. 2012.

[43] D. Caratelli, A. Yarovoy, and L. P. Ligthart, "Full-wave analysis of cavity-backed resistively loaded bow-tie antennas for GPR applications," in *Proc. Eur. Radar Conf.*, Oct. 2008, pp. 204–207.

[44] A. Taflove and S. C. Hagness, *Computational Electrodynamics: The Finite Difference Time Domain Method*. Norwood, NY, USA: Artech House, 2005.
[45] D. Caratelli, M. C. Viganó, G. Toso, P. Angeletti, A. A. Shibelgut, and R. Cicchetti, "A hybrid deterministic/metaheuristic synthesis technique for non-uniformly spaced linear printed antenna arrays," *Prog. Electromagn. Res.*, vol. 142, pp. 107–121, 2013. doi: 10.2528/PIER13071106.
[46] A. S. Nemirovsky and D. B. Yudin, *Problem Complexity and Method Efficiency in Optimization*. Hoboken, NJ, USA: Wiley, 1983.
[47] M. M. Khodier and C. G. Christodoulou, "Linear array geometry synthesis with minimum sidelobe level and null control using particle swarm optimization," *IEEE Trans. Antennas Propag.*, vol. 53, no. 8, pp. 2674–2679, Aug. 2005.
[48] Intel Corporation. *Core i7 Processors*. Accessed: May 2, 2019. [Online]. Available: http://www.intel.com/
[49] M. I. Skolnik, *Radar Handbook*. New York, NY, USA: McGraw-Hill, 1970.
[50] J. C. Curlander and R. N. McDounough, *Synthetic Aperture Radar, Systems and Signal Processing*. Hoboken, NJ, USA: Wiley, 1991.
[51] Y. K. Chan and V. C. Koo, "An introduction to synthetic aperture radar (SAR)," *Prog. Electromagn. Res. B*, vol. 2, pp. 27–60, Sep. 2008.
[52] J. S. Seybold, *Introduction To RF Propagation*. Hoboken, NJ, USA: Wiley, 2005.
[53] D. Caratelli, "Incomplete Anger-Weber functions: A class of special functions for electromagnetics," *Radio Sci.*, vol. 54, no. 4, pp. 331–348, 2019.
[54] W. L. Stutzman and G. A. Thiele, *Antenna Theory and Design*. Hoboken, NJ, USA: Wiley, 1997.
[55] D. Liu, U. Pfeiffer, J. Grzyb, and B. Gaucher, *Advanced Millimeter-Wave Technologies: Antennas, Packaging and Circuits. Chichester*. Hoboken, NJ, USA: Wiley, 2009.

Diego Caratelli (SM'19) was born in Latina, Italy, in 1975. He received the Laurea *(summa cum laude)* and Ph.D. degrees in electronic engineering and the M.Sc. degree *(summa cum laude)* in applied mathematics from the Sapienza University of Rome, Rome, Italy, in 2000, 2004, and 2013, respectively.

From 2005 to 2007, he was a Research Fellow with the Department of Electronic Engineering, Sapienza University of Rome. From 2007 to 2013, he was a Senior Researcher with the International Research Center for Telecommunications and Radar, Delft University of Technology, Delft, The Netherlands. In 2013, he co-founded The Antenna Company, Eindhoven, The Netherlands, where he is currently the Chief Technology Officer and is responsible for the technical direction, product development, program portfolio management, and coordination of the engineering team. Since 2015, he has been an Associate Professor with the Institute of Cybernetics, Tomsk Polytechnic University, Tomsk, Russia, and a Visiting Researcher with the Group of Electromagnetics in Wireless Telecommunications, Eindhoven University of Technology, Eindhoven, The Netherlands. He has authored or coauthored more than 190 publications in international peer-reviewed journals, book chapters, and conference proceedings. He holds 12 families of patents in antenna-related technologies and advanced computational techniques. His current research interests include the full-wave analysis and design of passive devices and antennas for satellite, wireless, and radar applications, the development of analytically based numerical techniques devoted to the modeling of wave propagation and diffraction processes, and the theory of special functions for electromagnetics, the deterministic synthesis of sparse antenna arrays, and the solution of boundary-value problems for partial differential equations of mathematical physics.

Dr. Caratelli has been a member of the IEEE Technical Committee TC-34 on Nanotechnology in Instrumentation and Measurement of the IEEE Instrumentation and Measurement Society since 2014 and is currently a member of ACES and Italian Electromagnetic Society (SIEm). He was a recipient of the Young Antenna Engineer Prize at the 32th European Space Agency Antenna Workshop and the 2010 Best Paper Award from the Applied Computational Electromagnetics Society (ACES). He was a co-recipient of the Frost and Sullivan Best Practices Award for technology innovation in advanced antennas for wireless communications in 2016.

Giovanni Toso (SM'07) received the Laurea *(cum laude)* and Ph.D. degrees from the University of Florence, Florence, Italy, in 1992 and 1995, respectively.

In 1996, he was a Visiting Scientist with the Laboratoire d'Optique Electromagnétique, Marseille, France. In 1999, he was a Visiting Scientist with the University of California at Los Angeles (UCLA), Los Angeles, CA, USA. In 2000, he has been appointed as a Researcher in a Radio Astronomy Observatory of the Italian National Council of Researches (CNR). Since 2000, he has been with the Antenna and Submillimeter Waves Section, European Space and Technology Centre, European Space Agency, Noordwijk, The Netherlands. He has been initiating and contributing to several research and development activities on satellite antennas based on arrays, reflectarrays, discrete lenses, and reflectors. In particular, in the field of onboard satellite antennas, he has been coordinating activities on multibeam antennas (active and passive) mainly for Telecom Applications. In the field of terminal antennas for Telecom Applications, he has been initiating several research and development activities on reconfigurable antennas with electronic, mechanical, and hybrid scanning. He has been coauthoring the best paper at the 30th ESA Antenna Workshop and the most innovative paper at the 30th and 36th ESA Antenna Workshops. He holds about 20 international patents.

Dr. Toso received, together with Prof. A. Skrivervik, the Best Teacher Award of the European School of Antennas (ESoA), in 2018. In 1999, he also received the Post-Doctoral Fellowship from the University of Florence and a Scholarship from Alenia Spazio, Rome, Italy. In 2018, he was the Chairman of the 39th ESA Antenna Workshop on Multibeam and Reconfigurable Antennas. In 2009, he was a Co-Editor of the Special Issue on Active Antennas for Satellite Applications in the *International Journal of Antennas and Propagation*. In 2014, he was a Guest Editor, together with Dr. R. Mailloux, of the Special Issue on Innovative Phased Array Antennas Based on Non-Regular Lattices and Overlapped Subarrays in the IEEE TRANSACTIONS ON ANTENNAS AND PROPAGATION, and for the same society, he was an Associate Editor from 2013 to 2016. Since the first edition in 2006, he has been significantly contributing to the ESoA course on satellite antennas. Since 2010, together with Dr. P. Angeletti, he has been instructing short courses on multibeam antennas and beamforming networks during international conferences, such as the IEEE Antennas and Propagation Society, the IEEE Microwave Theory and Techniques Society, the IEEE International Conference on Wireless Information Technology and Systems, the European Conference on Antennas and Propagation, and European Microwave Week, which have been attended by more than 600 participants.

Oleg V. Stukach (SM'01) received the Diploma degree (Hons.) in radio engineering and the Dr.Tech.Sci. degree in modeling, numerical methods, and software from the Tomsk State University of Control Systems and Radioelectronics, Tomsk, Russia, in 1988 and 2010, respectively.

In 1988, he joined the Picosecond Technique Labs, Tomsk. He is currently a Professor and the Chair of the Department of Computer-Aided Measurement Systems and Metrology, Tomsk Polytechnic University, Tomsk. He has authored or coauthored more than 200 technical papers and patents in the fields of microwave technique, ground penetrating radar (GPR), and theory of control. His current research interests include the theory of parametric invariance of nonlinear systems.

Dr. Stukach was a recipient of the Tomsk Region Prize in science and education. He is an Organizer and an active participant of international scientific conferences. He has been the Chair of the Biennial International Siberian Conference on Control and Communications (SIBCON) since 1995.

Nikolay V. Panokin received the Diploma degree in radio engineering from the Moscow Institute of Physics and Technology (MIPT), Moscow, Russia, in 1980 and the Ph.D. degree in electrodynamics theory and adaptive signal processing in phased arrays from Almaz Central Marine Design Bureau, Moscow, in 1986.

Since 2012, he has been the Head of Science Department, National University of Science and Technology MISiS, Moscow. His area of specialization and research interests include neural and intelligent signal processing, machine learning, pattern recognition, and radar imaging technology.